Physicochemical and functional properties of the muscle protein fraction of *Hypomesus olidus*

Yuan Fu [a], Chuanhao Liu [b], Xiaohui Yan [c], Guochuan Jiang [a], Qiao Dang [a], Liyan Wang [a,*], Xuejun Liu [a,*]

[a] College of Food Science and Engineering, Jilin Agricultural University, No. 2888 Xincheng Street, Changchun 130118, China
[b] Exyte Shanghai Co., Ltd., Shanghai, China
[c] Finance and Taxation College, Jilin Business and Technology College, No. 1666, Kalun Lake Street, Changchun 130102, Jilin, China

ARTICLE INFO

ABSTRACT

The physicochemical and functional properties of myofibrillar protein (MP), sarcoplasmic protein (SP), and myostromin (MY) in *Hypomesus olidus* muscle were evaluated and reported in this study. These fractions are rich in Glu. Three proteins exhibited significantly different morphologies, colors, and particle sizes. The main protein bands of MP, SP, and MY are 15–220 kDa, 26–60 kDa, and 15–245 kDa, respectively. In particular, MP is more hydrophobic. Three proteins exhibited a maximum UV absorption peak at 270 nm, and all amide I secondary structures were shown to be composed of repetitive units (e.g., α-helices and β-sheets). The three proteins demonstrated a predominantly amorphous halo, with T_d values of 52.22 °C, 59.16 °C, and 58.09 °C. Regarding their properties in water/oil absorption, emulsification, and foaming, MP is the most preferred, followed by SP and MY. In conclusion, *Hypomesus olidus* muscle proteins are novel and potential functional nutrition ingredients for the food industry.

Introduction

Fish are a food source with high protein content and can be used as an efficient meat replacer in highly carnivorous countries because they impose less environmental pressure than other consumable meat sources (Boer, Schsler, & Aiking, 2020). Proteins in fish muscle can be divided into 3 categories, namely, myofibrillar protein (MP), sarcoplasmic protein (SP) and myostromin (MY). All three categories contain all essential amino acids (AA), specifically Lys, Trp, His, Phe, Leu, Ile, Thr, Met-Cys, and Val.

Hypomesus olidus is a species in Salmonidae and is a small commercial freshwater fish primarily distributed in northeastern China, Korea, Japan, and northern Canada (Cho, Sohn, Shin, Song, & Choi, 2006). Relevant studies have shown that *Hypomesus olidus* is rich in protein with a useful composition of essential amino acids. Currently, fish are either frozen, processed or utilized fresh in most cases (Ceng, & Liu, 2014). Common cooked products include grilled fish fillets (Ceng, & Liu, 2014). However, these applications all pose certain problems, such as a small processing scale, low protein utilization rate, low processing extent, and low added value for products (Tang, Zhou, Hong, & Liu,

2011). The main forms of aquatic protein processing in China and abroad are frozen surimi (Shen et al., 2022) and surimi products (Shen et al., 2022), protein hydrolysates (Heffernan, Giblin, & O'Brien, 2021), feed fish meal (Sahar et al., 2022), etc., which have shortcomings such as low raw material utilization and environmental pollution.

Scientists have performed extensive studies on this topic in *Ctenopharyngodon idella* (Cho, Sohn, Shin, Song, & Choi, 2006)*, Oreochromis mossambicus* (Tang, Zhou, Hong, & Liu, 2011)*, Andrias davidianus* (Yang, Chen, Chen, & Dong, 2020) and so on*.* However, investigations on the muscle proteins in *Hypomesus olidus* are limited to chemical composition, nutritional qualities, extraction methods, and anticoagulation (Gou, Wang, & Liu. 2017). In other words, physicochemical and functional studies on the muscle protein fractions of *Hypomesus olidus* have been insufficient.

Therefore, it is very important to carry out basic research for better deep processing and exploitation of male pond marsh fish protein. Compared to the in-depth studies on the structure and properties of milk proteins (Mu et al., 2022) and plant proteins (Du et al., 2022), relatively few studies have been conducted on the isolation of fish protein systems and their properties. Currently, the most efficient method to prepare fish

protein to be used in the food industry is enzymatic hydrolysis (Heffernan, Giblin, & O'Brien, 2021). Many domestic and foreign studies on the enzymatic hydrolysis of fish protein have accumulated considerable technical experience in the preparation of hydrolyzed fish protein using enzymatic methods. However, the functional properties of hydrolyzed fish protein are poor, and the flavor itself is not good. In particular, poor dispersion, strong hygroscopicity and fishy taste and bitterness are especially important problems to overcome in order to meet the needs of successful food processing for wide use in the food industry.

The functional properties of fish proteins in modern fish processing technology are attracting increasing attention and not only affect the organoleptic properties of fish proteins, but also play important roles in their physicochemical properties in the manufacture, processing or preservation of food and feed. To make fish proteins better processed and utilized, there is an urgent need to address the core issue of protein research: the structure–function relationship.

Therefore, in this study, for the first time, male pond marsh fish proteins were separated according to the differences in solubility of each protein fraction and studied with respect to their colors, particle sizes, amino acid compositions, surface hydrophobicity (H_0), sulfhydryl group (SH) and disulfide bond (SS) contents, thermal properties, UV spectra, secondary structures, X-ray diffraction (XRD) features, sodium dodecyl sulfate–polyacrylamide gel electrophoresis (SDS-PAGE) features, scanning electron microscope (SEM) features, solubility, water holding capacity (WHC), oil holding capacity (OHC), emulsifying activity index (EAI) and emulsion stability index (ESI), as well as foaming capacity and foam stability (FC and FS), which were studied in a comprehensive and systematic manner. The aim was to provide a theoretical basis for the high-value processing and utilization of male pond marsh fish protein resources and the in-depth study of fish protein structure–function.

Materials and methods

Materials

Freshly dead *Hypomesus olidus* organisms were collected from the Aquatic Product Market in Changchun City, Jilin Province, China. They were refrigerated as soon as possible and transported to the laboratory within 6 h. In the food pretreatment laboratory, the fish were deboned, peeled and eviscerated to obtain complete fish muscles and then stored at -20 °C prior to use. All experiments were carried out in accordance with the animal experiment guidelines of Jilin Agricultural University. The protocol was approved by the Animal Protection and Use Committee of Jilin Agricultural University. The approximate compositions of *Hypomesus olidus* muscle were measured, including moisture (76.98 % $\pm$ 0.15), ash (0.93 % $\pm$ 0.04), protein (15.40 % $\pm$ 0.04), and lipid contents (3.34 % $\pm$ 0.03). All chemicals and reagents were of analytical grade and were obtained from Changchun Yibo Biotechnology Co., ltd.

Methods

Extraction of protein isolates from Hypomesus olidus muscle

Extraction of muscle protein isolates from *Hypomesus olidus* was performed following the procedures proposed by Saito (1983) with some modifications. Fifty grams of *Hypomesus olidus* muscle surimi was added to 4 × PBS buffer (0.05 mol·L^{-1}, pH 7.5) in an ice bath. Subsequently, the mixture was homogenized at 10,000 rpm/min for 2 min (homogenization for 30 s followed by intermittent pauses of 30 s, 2 rounds) and centrifuged at 4 °C and 8,000 r/min for 20 min. Following centrifugation, supernatant I was collected, and precipitate I was mixed with 4 × PBS buffer (0.05 mol·L^{-1}, pH 7.5) again to obtain supernatant II. After combining supernatants I and II, the combination was mixed with 4 × 5 % TCA (i.e., for every 1 mL of combination, 4 mL 5 % TCA was added), and the mixture was centrifuged after standing at room temperature for 1 h. The precipitate obtained after this centrifugation step was water-soluble sarcoplasmic proteins (SP). Subsequently, residue II extracted

from SP was mixed with 4 × PBS buffer (pH 7.5, including 1.1 mol·L^{-1} KCl) in an ice bath, followed by homogenization at 10,000 rpm/min for 2 min (homogenization for 30 s followed by intermittent pauses of 30 s, 2 rounds) and centrifugation at 4 °C, 8,000 r/min for 20 min to obtain residue III and supernatant III. Similar procedures performed with residue II were repeated for residue III to obtain residue IV and supernatant IV. Supernatants III and IV were combined as salt-soluble myofibrillar proteins (MPs), while the remaining residue V was insoluble myostromin (MY).

Protein desalination was performed with an MD77 (10,000 Da) dialysis bag. The bag was boiled with water for 10 min before placing the proteins inside for dialysis in a beaker filled with pure water (4 °C). The dialysate was replaced once every 4 h. The existence of chloride ions was tested by 1 g/100 mL AgNO$_3$ solution. When no chloride ions were detected, dialysis ended, and the obtained proteins were freeze-dried in a vacuum.

Color

The colors of MP, SP, and MY obtained in this study were observed with a HunterLab ColorFlex system following the method proposed by Nieves, María, María, & Ramon (2022) with small modifications. Three color components were observed, namely, L* (- black to + white), a* (- green to + red), and b* (- blue to + yellow).

Particle sizes

The particle sizes of the MP, SP, and MY protein fractions of *Hypomesus olidus* muscle were detected with a BT-9300HT laser diffraction particle size distribution analyzer (Dandong City Baxter Instrument Co. ltd.). The particle size distributions, as well as D_{10}, D_{50}, and D_{90}, were obtained. Specifically, D_{10}, D_{50}, and D_{90} were defined as 10 %, 50 %, and 90 % of the particle sizes within the measured size range, respectively.

Amino acids

One-hundred muscle protein isolates from *Hypomesus olidus* were transferred to and mixed well with 8 mL of 6 M HCl, vortexed for 5 s, and purged with nitrogen gas for 5 min. The sample tubes were sealed, transferred to an oven set at 110 °C, and heat insulated for 24 h for protein hydrolysis. After that, the samples were air-cooled, and a certain amount of ultrapure water was added before being evaporated to dryness. This procedure was repeated 3–5 times. Next, the samples were mixed with a fixed volume of ultrapure water before being filtered through a 0.22 μm microporous filter membrane. The filtered samples were combined with a certain amount of buffer solution and a derivatization reagent and sealed for subsequent derivatization at 55 °C for 10 min. Finally, the samples after derivatization were transferred into automatic sampling vials for UPLC measurements.

Surface hydrophobicity (H_0)

In this study, the H_0 values of MP, SP, and MY were measured by the method proposed by Mune & Sogi (2016) with small modifications. Bromophenol blue was used to reflect H_0. First, MP, SP, and MY were diluted to 2 mg·mL^{-1} with PBS buffer (20 mmol·L^{-1}, pH 6.0). One milliliter of MP, SP, and MY solution was mixed with 200 μL of 1 mg·mL^{-1} bromophenol blue solution and allowed to react at 25 °C for 10 min before centrifugation at 3,000 rpm/min for 15 min. The supernatant was diluted 10-fold and the absorbance was measured at 595 nm with phosphate buffer as the blank control. Subsequently, H_0 was calculated according to the following formula:

$$H_0(\%) = \text{BPB bound/ug} = 200(A_0 - A)/A_0 \tag{1}$$

where A_0 is the absorbance of the blank control and A is the absorbance of the sample.

Sulfhydryl groups (SH groups) and disulfide bonds (SS)

The contents of sulfhydryl groups (SH groups) and disulfide bonds

(SS) in MP, SP, and MY were measured according to the method proposed by Brishti, Yea, Muhammad, Ismail-Fitry & NSaari (2020).

Thermal properties

The thermal properties of MP, SP, and MY were measured with a differential scanning calorimeter (DSC-Q20, TA Instruments, New Castle, Delaware, USA) with some modifications. Twenty milligrams of MP, SP, and MY samples were accurately weighed and sealed in an aluminum pan for heat scanning (20–120 °C at a heating rate of 10 °C/min). The peak denaturation temperatures (T_d) and denaturation enthalpy (ΔH) were measured.

UV spectra

UV spectra of the MP, SP, and MY samples were measured. MP, SP, and MY sample suspensions at 2 mg·mL^{-1} prepared with 0.05 mol·L^{-1} Tris-HCl buffer (pH 8.0) were centrifuged at $3,900 \times g$ for 20 min. Then, the supernatants were scanned by a UV–Vis spectrophotometer (Perkin Elmer, UV/VIS Lambda 365, America) over 250–360 nm at a rate of 10 nm/min.

Secondary structures

Fourier transform infrared spectroscopy (FTIR) was performed with sample powders (1 mg) embedded in KBr flakes (200 mg) to obtain the FTIR spectra of MP, SP, and MY within 4000–400 cm^{-1}. The amide I absorbance data (1600 cm^{-1}-1700 cm^{-1}) were then chosen to exhibit the secondary structure elements of the proteins. OMNIC 9.2 (Thermo Fisher Scientific, WI, USA) and 2018 (OriginLab Corporation, Northampton, MA, USA) software were used to perform baseline correction at 1600–1700 cm^{-1}, and Gaussian fractional peak fitting was used to calculate the relative percentages of each secondary structure component based on its integral area in the second derivative spectrum (Chen, Ma, & Fu, 2019).

X-ray diffraction (XRD) measurements

The XRD spectra of MP, SP, and MY were measured following the method of Li, Wang, Zheng, & Guo (2020) with some modifications. XRD spectra were obtained with a Rigaku SmartLab SE instrument (Rigaku Corporation, Japan) for physical structure analysis with copper Kα radiation at 40 kV and 40 mA. XRD scans were performed with $2\theta = 15°$-$45°$ and an angular speed of 2°/min.

Sodium dodecyl sulfate–polyacrylamide gel electrophoresis (SDS-PAGE)

SDS–PAGE results of MP, SP, and MY were obtained following the method of Yang, Chen, Chen, & Dong (2020) with some modifications. Briefly, MP, SP, and MY were mixed with a sample buffer to obtain a final protein concentration of 2 mg·mL^{-1}. SDS-PAGE was conducted in a 5 % acrylamide stacking gel (40 % acrylamide-bisacrylamide, 10 % SDS, 1 M Tris-HCl, pH 8.8, 10 % ammonium persulfate, TEMED) and subsequent 12 % separating gel (40 % acrylamide-bisacrylamide, 10 % SDS, 1 M Tris-HCl, pH 6.8, 10 % ammonium persulfate, TEMED).

Scanning electron microscope (SEM) observations

SEM observations of MP, SP, and MY were obtained following the method of Liu, Wang, Xue, & Benu (2022) with some modifications. Scanning electron microscopy (JSM-5200, Jeol Ltd., Tokyo, Japan) was used to observe the surface characteristics of MP, SP, and MY powders at an accelerating voltage of 15 kV. Each sample was deposited directly on the aluminum root, carbon conductive tape was bonded on both sides, and the gold layer was coated by gold sputtering before observation. Specifically, micrographs were taken at 2.5 k× and 1.0 k× magnifications.

Solubility

The percent protein solubility (PPS) of MP, SP, and MY was measured following the method of Shen, Gao, Xu, Ohm, & Chen (2020) with some modifications. Briefly, the pH of the 0.1 % protein suspension

was adjusted to 2–10 with either 0.1 M HCl or 0.1 M NaOH, and the sample solution was centrifuged (8,000 r/min) for 15 min. The protein concentration in the supernatant was detected by a Pierce™ BCA protein detection kit. In particular, to determine the total protein content, the fish protein isolates were dissolved in 0.1 M NaOH at 0.1 wt%, and PPS was calculated with the following equation:

$$PPS(\%) = protein\ content\ in\ the\ \text{su}pernatant/total\ protein\ content \times 100\%$$

(2)

Water holding capacity (WHC)

The WHC values of MP, SP, and MY were measured based on the method of Li et al., 2022 with some modifications. Briefly, 0.1 g MP, SP, or MY (dry basis) was added to preweighed test tubes and vortexed with 5 mL distilled water (Vortex-QL-901, Kylin-Bell Lab Instruments, China) for 30 s. After that, the solution stood at room temperature (25 °C) for 30 min and was centrifuged at 3,000 rpm for 25 min. The supernatant was then decanted carefully. The weights of test tubes containing postdecanting samples were compared with those of the test tubes containing dry-basis sample proteins in the beginning. The results were reported as grams of water absorbed per gram of protein sample.

Oil holding capacity (OHC)

The OHC values of MP, SP, and MY were measured according to the method of Zhu et al., 2022 with some modifications. Briefly, 0.1 g MP, SP, or MY (dry basis) was added to preweighed test tubes and vortexed with 5 mL mustard oil (Vortex-QL-901, Kylin-Bell Lab Instruments, China) for 30 s. After that, the solution stood at room temperature (25 °C) for 30 min and was centrifuged at 3,000 rpm for 25 min. The supernatant was decanted carefully. The weights of test tubes containing postdecanting samples were compared with the initial weights of the test tubes containing dry-basis sample proteins. The results were reported as grams of oil absorbed per gram of protein sample.

Emulsifying activity index (EAI) and emulsion stability index (ESI)

The EAI and ESI of MP, SP, and MY were determined based on the method of Yang et al., 2022 with some modifications. Briefly, 45 mL 0.2 % (w/v) protein isolate solutions and 15 mL mustard oil were homogenized in a beaker with a home blender for 3 min to create an emulsion. Subsequently, 50 μL of the emulsion was pipetted from the bottom of the homogenized emulsion immediately after homogenization and diluted (1:100, v/v) in 0.1 % (w/v) SDS. Following a 5-second vortex, the absorbance of the diluted emulsion was observed at 500 nm (Perkin Elmer, UV/VIS Lambda 365, America). The absorbance values measured immediately (A_0) and 10 min (A_{10}) after emulsion formation were used to calculate EAI and ESI in the following equations.

$$EAI\left(m^2/g\right) = (2\ 2.303\ A_0 DF)/(c\varnothing(1-\theta)10,000)$$

(3)

$$ESI\ (min) = A_0 \Delta t/\Delta A$$

(4)

where DF is the dilution factor (1 0 0), c is the initial protein concentration (g·mL^{-1}), Φ is the optical path (0.01 m), θ is the fraction of oil used to form the emulsion (0.25), and A_0 is the absorbance of the diluted emulsions. Measurements were performed at least three times for both A_0 and A_{10}, and $\Delta A = A_0$-A_{10}, where $\Delta t = 10$ min.

Foaming capacity (FC) and foam stability (FS)

The FC and FS of MP, SP, and MY were measured according to the method of Cc, Cs, Hl, & Rs (2020) with some modifications. An aliquot (6 mL) of 0.5 % solution (w/v) was homogenized with an IKA T18 digital ULTRA-TURRAX (IKA, Germany) at 15,000 rpm for 2 min at room temperature to incorporate air. The homogenized sample was immediately transferred to a 25 mL test tube. The total volume was recorded 30 s later to calculate FC (%). Subsequently, the homogenized sample was allowed to stand for 10 min, and its volume was recorded again to calculate FS (%). The calculation equations for FC and FS are listed

below:

$$FC(\%) = (A_0 - B)/B \times 100\% \qquad (5)$$

$$FS(\%) = (A_t - B)/B \times 100\% \qquad (6)$$

where A_0 is the volume after homogenization (mL) and B is the volume before homogenization (mL).

Statistical analysis

All experiments in this research were carried out as completely randomized design tests. One-way analysis of variance (ANOVA) and Duncan's multiple range tests were used to determine the significant differences among the variables. Differences with a p value < 0.05 were considered significant, and all data are reported as the mean $\pm$ SD. All experiments were run in triplicate (n = 3).

Results and discussions

Colors and particle sizes

Table 1 shows the color parameters of the protein fractions in *Hypomesus olidus* muscle. Compared to SP and MY, MP demonstrated the highest L* value, which is reflected in its creamy white appearance. On the other hand, SP exhibited the highest a* and b* values among the three, suggesting that it contains a higher degree of redness and yellowness, which is reflected in its yellowish-red appearance. Finally, MY exhibited the lowest a* value, which could explain its creamy blue appearance. Similar results have been observed in catfish, Indian mackerel, pony fish, and sardine (Kumarakuru, Reddy, & Haripriya, 2018). In addition, the colors of fish protein isolates are partially dependent on the connective tissues and retained lipids, which may enhance the lightness and influence yellowness, respectively. Moreover, coprecipitation of heme proteins can affect redness (Shaviklo, Thorkelsson, & Arason, 2010), while denaturation and oxidation of hemoglobin could impart a yellow–brown color to products. Finally, the color parameters (Table 1) of MP, SP, and MY are consistent with the color image (Fig. 1).

Table 1 also shows the particle size parameters of protein fractions in *Hypomesus olidus* muscle. Specifically, MY demonstrated the highest D10, D50, and D90, followed by SP and MP. MP has the smallest particle size that allows a larger surface area to reflect more light, which explains its higher L* value than the other two proteins (Table 1, Fig. 1). Moreover, these three protein isolates are slightly larger than those in catfish (704.85 nm), Indian mackerel (1453.23 nm), pony fish (1957.32 nm), and sardine (584.01 nm) (Kumarakuru, Reddy, & Haripriya, 2018). One possible reason for such differences could be protein aggregation during precipitation or treatment steps in the isolation procedure. Finally, the particle sizes of MP, SP, and MY are consistent with the SEM image

Fig. 1. Color of protein fractions from *Hypomesus olidus* muscle. MP: myofibrillar protein, SP: sarcoplasmic protein, MY: myostromin.

(Fig. 6).

Amino acid compositions

The amino acid compositions of MP, SP, and MY, along with the reference requirements of essential amino acids (EAAs) for infants and adults (FAO/WHO, 2007), are displayed in Table 2. In particular, 17 types of amino acids were detected in MP, SP, and MY, including eight EAAs. Similar data were observed for tilapia muscle and protein fractions (Tang, Zhou, Hong, & Liu, 2011). The isolated proteins contained all essential amino acids (except Try), with MP, SP and MY accounting for 42 %, 35 % and 41 % of the total amino acid content, respectively. Therefore, all three MP, SP and MY can be considered high-quality natural proteins consisting of most essential amino acids. Among them, Glu, Asp and Leu are the main constituent amino acids of MP, SP and MY. The total contents of the three amino acids in MP, SP and MY were 240.45 mg·g^{-1}, 244.44 mg·g^{-1} and 122.07 mg·g^{-1}, respectively. High levels of flavor-related amino acids, such as Asp and Glu, may be responsible for the special flavor of *Hypomesus* olidus proteins. The differences in Glu and Thr between MP and SP were not statistically significant (p $>$ 0.05), the differences in lysine between SP and MY were not statistically significant (p $>$ 0.05), and there were significant differences in other amino acids between MP, SP and MY (p $<$ 0.05). This can be explained by their different genotypes.

The amino acid composition of samples could provide an understanding of their thermal stability. In fact, hydrophobic amino acids are responsible for a more compact interior core of the protein. A higher total amount of hydrophobic amino acids indicates more stable protein. The slight differences in the total amount of hydrophobic amino acids between MP (282.80 mg/100 g of protein), SP (240.25 mg/100 g of protein) and MY (109.61 mg/100 g) may contribute to reduced thermodynamic stability for *Hypomesus olidus*. In addition, the *Hypomesus olidus* muscle contained all EAAs at specified levels required by the FAO/WHO (2007) for infants and adults. The EAA composition of *Hypomesus olidus* muscle meets the minimum EAA requirement proposed by FAO/WHO (2007) for adults, making the muscle a good nutritional supplement.

Surface hydrophobicity (H_0)

Table 3 shows the H_0 data of MP, SP, and MY, where MP demonstrates the highest H_0 compared with the other two. This indicates that MP has good hydrophobicity. Similar results were observed for muscle proteins in *Esox lucius* (Liu, Tian, Tong, & Zhang, 2016). The H_0 differences among protein fractions across fish species may be explained by the varied levels of hydrophobic residues in the fractions and the exposure of these residues after processing or denaturation. This result could also be explained by their different total amounts of hydrophobic amino acids (Table 2).

On the other hand, MP shows higher surface hydrophobicity, which is consistent with MP's higher oil absorption capacity (Table 5), because proteins with high surface hydrophobicity easily align and bind their hydrophobic residues to the oil phase.

Sulfhydryl groups (SH groups) and disulfide bonds (SS)

Table 3 shows the contents of SH groups and SS of the three protein fractions in *Hypomesus olidus* muscle, where MP demonstrated the highest content of total/free SH groups among the three. Again, similar results have been reported in *Esox Lucius* (Liu et al., 2016). This may be due to the greater protein denaturation of MP, which leads to the expansion of the protein structure and reveals more SH groups. For the exposed SH content, the recorded value of MP is slightly higher than those of SP and MY. For MP, protein denaturation may be the result of freeze-drying. On the other hand, it may be due to differences in the protein amino acid composition of different components, which may be

partly reflected in the different number of amino acids containing sulfur groups (Mehdi & Ingrid, 2018). Table 2 shows that among the three components studied, the content of amino acids containing sulfur groups (Met and Cys) is the highest in MP, and the recorded value of MP is slightly higher than those of SP and MY.

In the freeze-drying process, the freezing and drying stress denature protein to a certain extent, the protein structure expands, the free sulf-hydryl groups are exposed, and the sulfhydryl groups are further oxidized to form SS bonds (Hu et al., 2010). The content of SS bonds is the highest in MP, followed by SP and MY. Combining this finding with those from surface hydrophobicity analysis, it could be concluded that higher contents of exposed hydrophobic groups would promote the formation of SS bonds from adjacent free SH groups, which would, in turn, lead to various degrees of interchange reaction and aggregation (Gong et al., 2016).

Thermal properties

The thermal denaturation temperatures and heat capacities of the different protein fractions studied in this report are also presented in Table 3. A single enthalpy peak was observed for all fractions. The T_d values for MP and SP were 52.22 °C and 59.16 °C, respectively: 52.22 °C was considered to be related with myosins because the thermal transition temperatures of typical myosins range from 38 °C to 67 °C (Chen et al., 2014). A similar denaturation temperature (59.3 °C, comparable to that of the SP found here) was found for the SP of *Gadus morhua* (Thorarinsdottir, Arason, Geirsdottir, Bogason, & Kristbergsson, 2002).

The T_d of MY, a myostromin, was 58.09 °C. Among all myostromins, collagen is the main protein component, accounting for 85.23 % of the total myostromin. According to literature reports, the denaturation temperatures of most fish, livestock, and poultry collagens are 56 °C to 62 °C (Martens, Stabursvik, & Martens, 1982).

Finally, both T_d (the denaturation temperature) and ΔH (the amount of input heat energy required to denature protein) can reflect the thermal stability of a protein. The ΔH value of MP (4.147 J·g^{-1}) was significantly higher (p < 0.05) than those of the SP (3.147 J·g^{-1}) and MY (2.019 J·g^{-1}). This result suggested that the structure of MP is more crystalline than those of SP and MY; thus, the energy required for its complete denaturation will be higher. The obtained finding confirmed the XRD analysis results. Proteins with an ordered and compact conformation showed greater thermal stability than unassociated proteins. Thus, MP exhibited better thermal stability than SP and MY. This result could be explained by their different total amounts of hydrophobic amino acids (Table 2).

UV spectra

The UV spectra of all the protein fractions investigated in this study are presented in Fig. 2. Peak wavelengths of MP, SP, and MY were observed from 265 nm to 300 nm, a wavelength range typical of fish proteins. These peaks were reported to be associated with tyrosine and tryptophan molecules. Therefore, these protein fractions from *Hypomesus olidus* contain tryptophan and tyrosine. Similar findings were also observed in the muscle proteins of *Andrias Davidianus* (Yang, Chen, Chen, & Dong, 2020). The UV spectra are determined to reveal consistent results with the amino acid study, and both would help predict the protein conformation.

Secondary structure

Fig. 3(A) displays the FTIR spectra of MP, SP, and MY. The broad band at 3416–3421 cm^{-1} is assigned to amide A, and the band at 2960–2962 cm^{-1} is assigned to amide B. Following that, the regions of 1644–1661 cm^{-1}, 1544–1553 cm^{-1}, and 1223–1243 cm^{-1} belong to amide I, amide II, and amide III groups, respectively. The amide II group is the combined result of N—H bending vibrations and C—N stretching
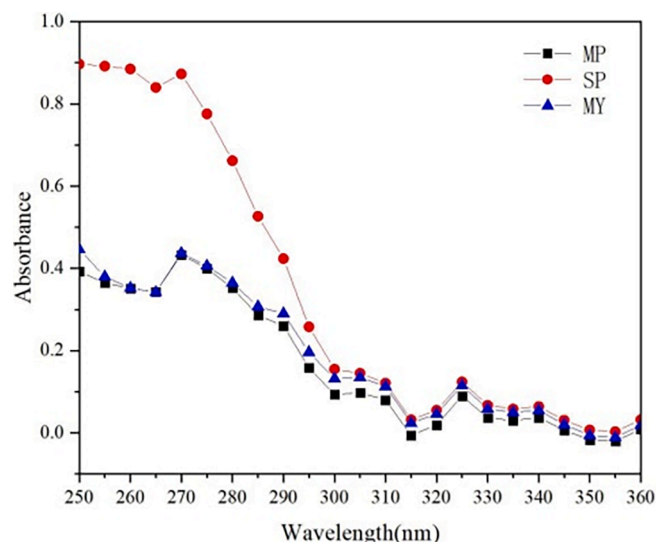

Fig. 2. UV spectra of protein fractions from *Hypomesus olidus* muscle. MP: myofibrillar protein, SP: sarcoplasmic protein, MY: myostromin.

vibrations. The amide III signal is caused by the combination of N—H bending vibration and C—N stretching vibration, as well as some minor contributions from C—O plane bending and C—C stretching vibration (Shevkani, Singh, Rana, & Kaur, 2014). In particular, the intensity of the amide I group signal was higher than those of amide II and amide III. Principally, the amide I group signal is the result of the superposition of several structural elements reflecting C—O vibrations (70–85 %) (Navarro-Lisboa et al., 2017). Therefore, the amide I group is frequently used to estimate the secondary structure.

As a common indicator of protein secondary structure, amide I absorption (1700–1600 cm^{-1}) represents the stretching vibration of the C=O bond. Five major peaks were identified from this curve, which corresponded to β-sheet (1610–1642 cm^{-1}), β-turn (1660–1680 cm^{-1}), β-antiparallel (1680–1700 cm^{-1}), α-helix (1650–1660 cm^{-1}), and random coil (1642–1650 cm^{-1}) motifs (Chen et al., 2019). As seen in Fig. 3 (B-MP), it was suggested that the peaks (1622.6 cm^{-1}, 1637.6 cm^{-1}, 1652.4 cm^{-1}, 1666.4 cm^{-1} and 1681.8 cm^{-1}) found in the spectra of MP corresponded to the β-sheet, α-helix, β-turn and β-antiparallel motifs mentioned above. As seen in Fig. 3 (E), the ranked order of contents is β-sheet (35 %) > α-helix (28 %) > β-turn (23 %) > β-antiparallel (14 %). As seen in Fig. 3 (C-SP), it was suggested that the peaks (1617.9 cm^{-1}, 1633.3 cm^{-1}, 1649.8 cm^{-1}, 1665 cm^{-1} and 1681.3 cm^{-1}) found in the spectra of SP corresponded to the β-sheet, random coil, β-turn and β-antiparallel motifs mentioned above. As seen in Fig. 3 (E), their relative contents are ranked as β-sheet (45 %) > random coil (25 %) > β-turn (19 %) > β-antiparallel (11 %). As seen in Fig. 3 (D-MY), it was suggested that the peaks (1621.7 cm^{-1}, 1635.7 cm^{-1}, 1651.5 cm^{-1}, 1667.1 cm^{-1} and 1683 cm^{-1}) found in the spectra of MY corresponded to the β-sheet, random coil, β-turn and β-antiparallel motifs mentioned above. As seen in Fig. 3(E), their ranked relative contents are β-sheet (38 %) > α-helix (26 %) > β-turn (24 %) > β-antiparallel (12 %). In general, α-helices are stabilized by intramolecular hydrogen bonds between the carbonyl oxygen (C=O) and amino hydrogen (NH–) groups on the polypeptide chain and are buried within the protein interior sites, while β-turns usually appear in highly ordered protein structures. Furthermore, random coils originate from the unfolding of any structure of higher order, and they are related to protein flexibility.

In conclusion, all protein fractions analyzed in this study demonstrate five typical motif structures, and their relative contents are ranked as β-sheet > α-helix/random coil > β-turn > β-antiparallel.
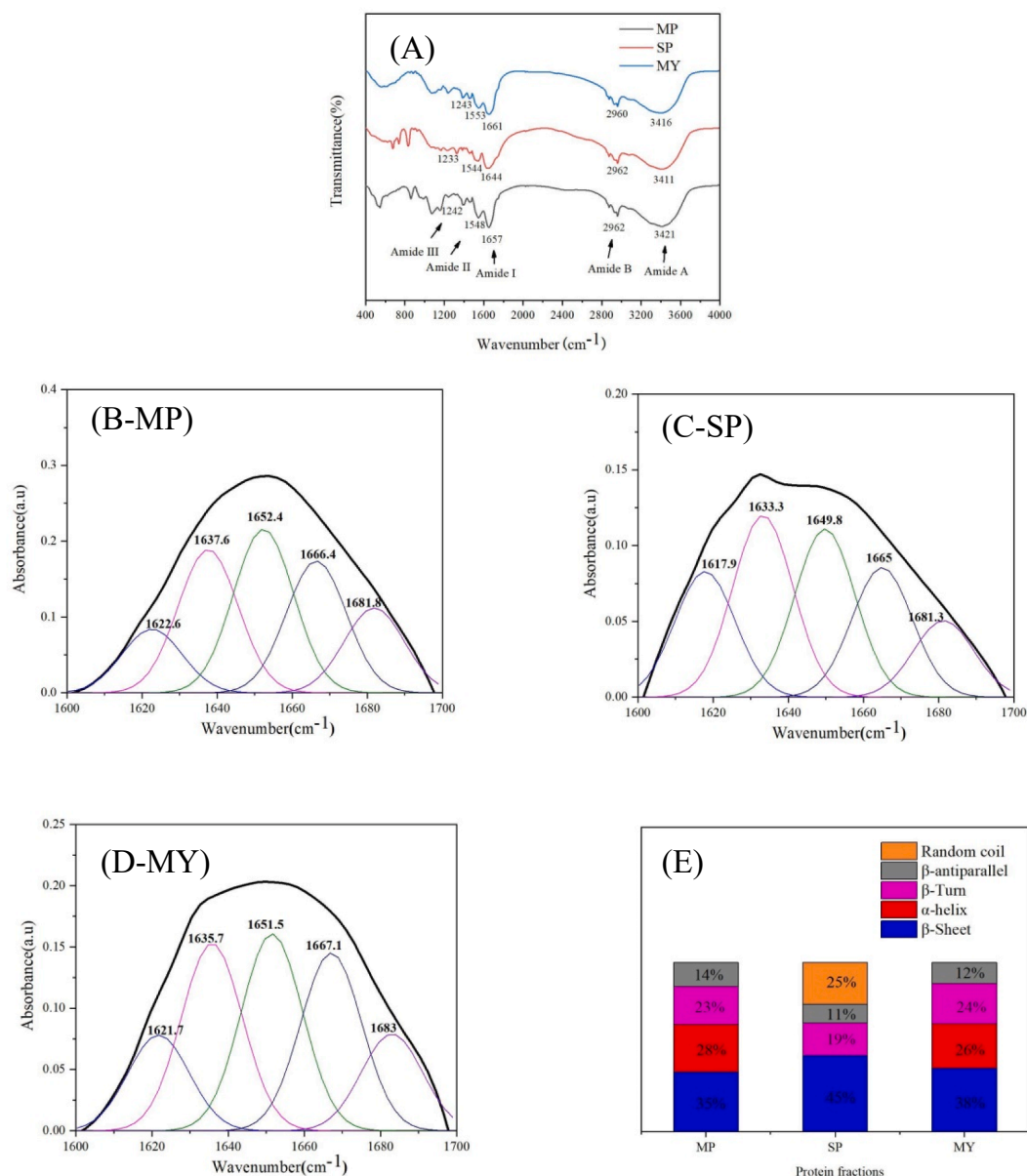
Fig. 3. (A) FTIR spectra for protein fractions from *Hypomesus olidus* muscle. (B-MP), (C-SP) and (D-MY) Illustration of the Gaussian deconvolution of the FTIR signal in the Amide I region.(E) Secondary structure of protein fractions from *Hypomesus olidus* muscle. MP: myofibrillar protein, SP: sarcoplasmic protein, MY: myostromin.

XRD

Typically, solid food materials can be crystalline, semicrystalline, or amorphous. The XRD patterns in Fig. 4 show that all samples displayed a predominantly amorphous halo or a wide band with a peak at $2\theta = 20°$. Similar peaks were also reported for myofibrillar proteins from golden threadfin bream (Li, Wang, Zheng, & Guo, 2020).

Proteins with more amorphous contents are generally considered to be more soluble and compressible (Ahmad et al., 2018). Therefore, the proteins in *Hypomesus olidus* demonstrate better solubility and compressibility. In addition, the three protein fractions exhibit close and very narrow peaks independent of each other, suggesting that crystallization or smectics exist in MP, SP, and MY. Moreover, the diffraction peaks are sharp, indicating perfect crystallization.

SDS-PAGE

The individual protein compositions of MP, SP, and MY were visualized by SDS-PAGE (Fig. 5). The MP samples showed a myosin heavy chain (MHC, 222 kDa), M−protein (160 kDa), α-actinin (90 kDa), actin (44 kDa), tropomyosin (35 kDa), and myosin light chains (MLC1-3, 23 kDa, 18 kDa, and 15 kDa), all of which were consistent with previous reports (Mignino & Paredi, 2006). The molecular weights of the major SP components were found to be 26–60 kDa, and an obvious protein band was observed, similar to a previous report. However, the relative molecular weight distribution of MY was wide, with bands ranging within 15–245 kDa. Specifically, the bands of 15–45 kDa and 60–245 kDa were the darkest, which might be the characteristic bands of alkali-soluble proteins and collagen.
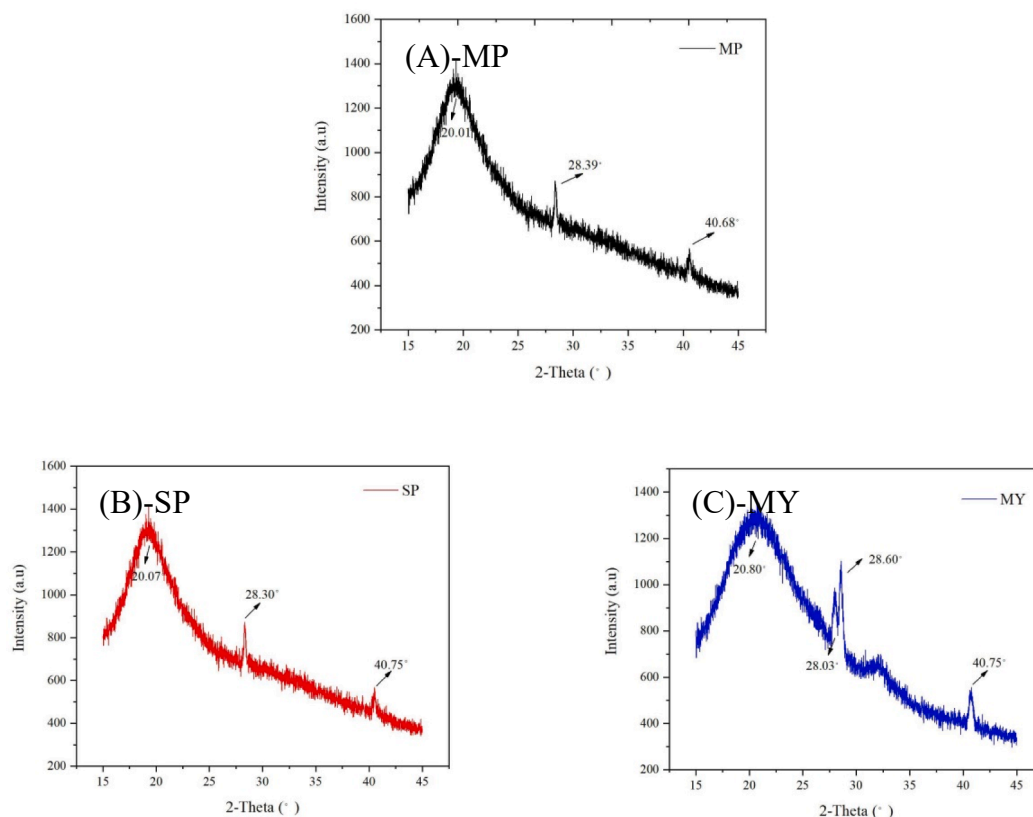
Fig. 4. X-ray patterns of protein fractions from *Hypomesus olidus* muscle. MP: myofibrillar protein, SP: sarcoplasmic protein, MY: myostromin.
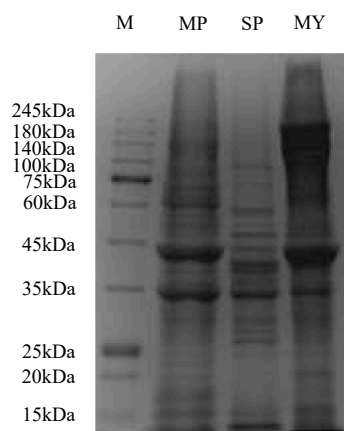

Fig. 5. SDS-PAGE profile of protein fractions from *Hypomesus olidus* muscle. MP: myofibrillar protein, SP: sarcoplasmic protein, MY: myostromin, M: represents protein molecular weight marker.

SEM

To more deeply understand the characteristic aggregation of MP, SP, and MY from *Hypomesus olidus*, SEM was applied to observe the morphology of the fractions (Fig. 6). Judging from Fig. 6, the three fractions demonstrate remarkable differences in their microstructures. In Fig. 6A-MP-1 and Fig. 6A-MP-2, the molecules were interconnected into spheroidal and rod-like aggregates of various sizes, confirming that MP oligomers and filaments are unstable and tend to form complex structures via hydrophobic interactions and hydrogen bonds. Similar structures were observed in milk protein concentrate (Shilpashree, Arora, Chawla, & Tomar, 2015). SP revealed smooth and regular

surfaces as well as smooth and compact protein bundles (Fig. 6B-SP-1 and Fig. 6B-SP-2). Finally, Fig. 6C-MY-1 and Fig. 6C-MY-2 reveal mostly connective tissues with relatively complete fiber structures.

Solubility

The protein solubility of the MP, SP, and MY samples as a function of pH is summarized in Table 4. The solubility values of MP, SP, and MY at pH = 7 were 21.19 %, 28.24 %, and 14.55 %, respectively, all of which are higher than that of hake protein powder (4 %) (Pires et al., 2012). Such differences could be explained as a result of different species. When increasing the solution pH to 10, the solubility of MP, SP, and MY increased to 46.88 %, 44.95 %, and 43.20 %, respectively, all of which are considerably higher than the value for herring protein (29 %) (Mehdi & Ingrid, 2018). Such variation could be the result of varied extraction methods.

In general, MP and MY are very insoluble at pH = 5, and SP is barely soluble at pH 6. Denaturation during shifts in pH might affect the solubility of the protein fractions. Previous studies have summarized that the aqueous solubility of proteins depends on multiple factors, including surface characteristics, molecular weights, and conformations. With comparable or greater solubility than most other proteins, the MP, SP, and MY in *Hypomesus olidus* may have great application prospects in food products.

Water/oil holding capacity (WHC/OHC)

As shown in Table 5, the WHC of MP, SP, and MY was 2.30–4.40 mL·g^{-1}, which is comparable with that of tilapia fish proteins (2.63 mL·g^{-1}) (Foh, Wenshui, Amadou, & Jiang, 2012). The amino acid composition, conformation, hydrophobicity, pH, temperature, ionic strength, and concentration of proteins are reported to be closely related to the quantity of water they contain. Proteins with desirable WHC
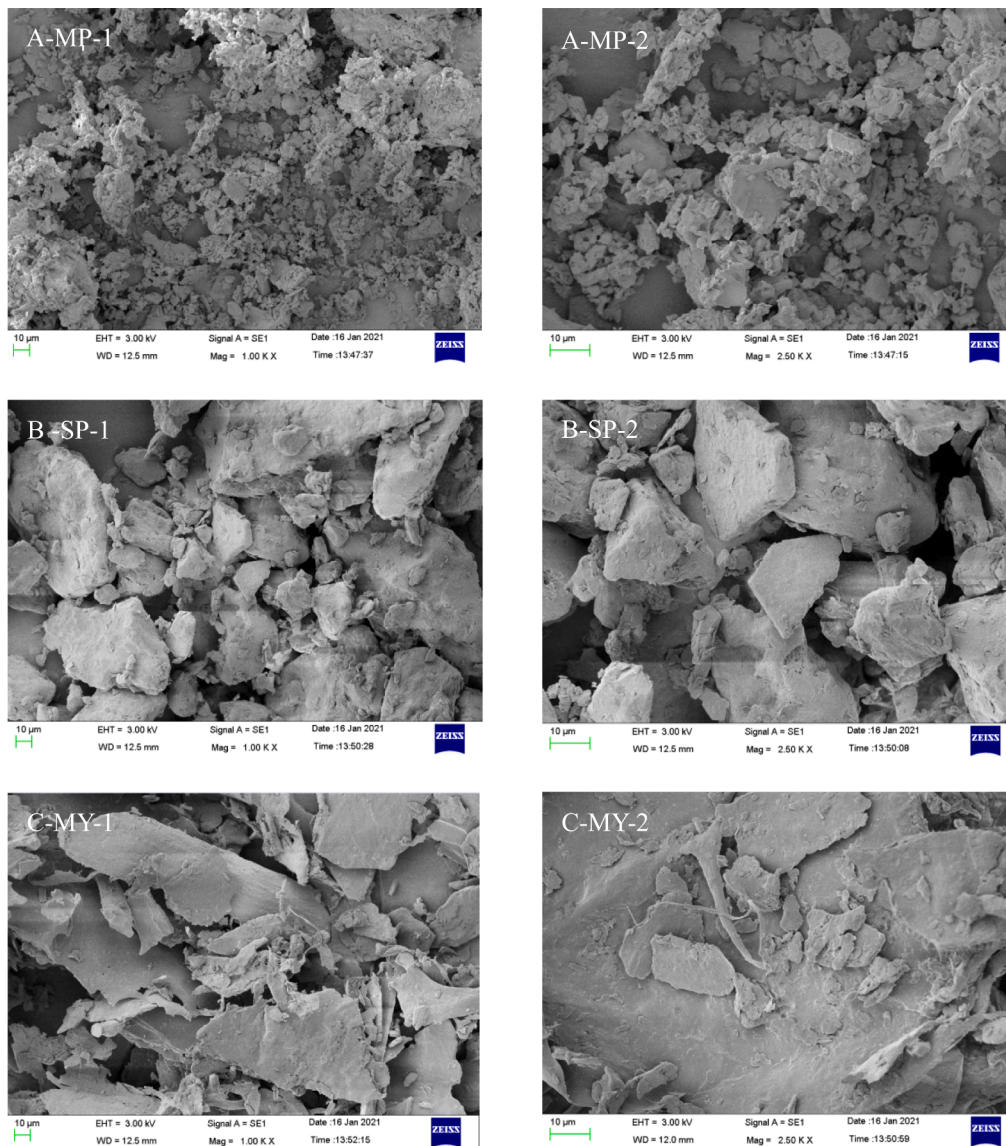
Fig. 6. SEM images of protein fractions from *Hypomesus olidus* muscle. A-MP: myofibrillar protein, B-SP: sarcoplasmic protein, C-MY: myostromin (1: ×1.00KX, 2: ×2.50KX).

values could be used as promising additives in comminuted meats, baked doughs, bakery products, sausages, and gels.

On the other hand, the OHC reflects the capacity of food materials to absorb oil. In this study, MP, SP, and MY were revealed to have varied OHC values of 5.70 mL·g^{-1}, 4.40 mL·g^{-1}, and 3.4 mL·g^{-1}, respectively. Although their mutual differences are significant ($p < 0.05$), the OHC values of MP, SP, and MY in this study are still higher than those in tilapia fish proteins (3.38 mL·g^{-1}) (Foh et al., 2012). The OHC of food materials is affected by the type and amount of proteins, degree of hydrolysis, temperature, type of oil, etc. Proteins with high OHC numbers could be used in food industries as additives in ground meat formulations, meat substitutes, extenders, doughnuts, soups, sausages, baked products, cake batters, mayonnaises, and salad dressings.

Emulsifying activity index (EAI) and emulsion stability index (ESI)

The EAI and ESI values of the protein fractions in *Hypomesus olidus* muscle are presented in Table 5. The EAI is an indicator of the ability of proteins to act as interfacial active agents in an oil-in-water interface. The EAI values of MP, SP, and MY were 159.19 m^2·g^{-1}, 124.72 m^2·g^{-1}, and 65.80 m^2·g^{-1}, respectively, and their mutual differences were

significant ($p < 0.05$). All of these values are similar to those in tilapia muscle (Tang, 2011). SP and MY are expected to show a lower EAI than MP since they also demonstrate lower SH and solubility, which are two indicators of EAI. Generally, greater protein solubility and surface hydrophobicity would lead to lower interfacial tension and better emulsification.

ESI reflects how long an emulsifier can keep the dispersed oil droplet in a solution stable to withstand perturbation to its structure (e.g., coalescence, creaming, flocculation, and sedimentation). The ESI values of MP, SP, and MY were 15.15 min, 16.62 min, and 26.14 min, respectively, with significant mutual differences ($p < 0.05$). All of these values are similar to those in tilapia muscle (Tang, 2011). It could be concluded from the previous analysis that EAI and ESI vary across fractions, which is possibly due to different physicochemical properties (i.e., surface hydrophobicity and solubility).

Foaming capacity and foam stability (FC and FS)

The FC and FS of the *Hypomesus olidus* protein fractions are presented in Table 5. The interfacial area a protein can produce is referred to as FC, and FS denotes the capability of a protein to stabilize air bubbles against

gravitational stress. The FC numbers of MP, SP, and MY were up to 110 %, 87 %, and 78 %, respectively, and the mutual differences were significant (p < 0.05). For FS, the numbers became 58 %, 88 %, and 98 % for MP, SP, and MY, respectively, with significant differences among the three (p < 0.05). These FC and FS values are similar to those obtained from tilapia muscle (Tang, 2011). Protein foaming is regulated by three major factors, namely, the transportation, penetration, and reorganization of molecules at the air/water interface. In addition, numerous factors, such as protein solubility, rigidity-flexibility equilibrium in proteins, pH, hydrophobicity, temperature, and ionic strength, could also affect FC and FS (Shevkani, Singh, Kaur, & Rana, 2015).

Conclusions

In summary, this study provides information about the physicochemical and functional properties of protein fractions (MP, SP, and MY) from the *Hypomesus olidus* muscle. The muscle of *Hypomesus olidus* is rich in amino acids. Compared with SP and MY, MP has higher surface hydrophobicity and sulfhydryl contents, as well as more disulfide bonds. All three protein fractions exhibited the maximum UV absorption peak at 270 nm, and the relative amounts of structural contents in their secondary structures were all ranked as β-sheet > α-helix/random coil > β-turn > β-antiparallel. In addition, MP, SP, and MY also demonstrate amorphous protein structure with high thermal stability. Compared with SP and MY, MP exhibits better solubility and greater water holding capacity, as well as higher emulsifying capacity and foaming capacity. Thus, the protein fractions from *Hypomesus olidus* muscle are desirable for food applications.

CRediT authorship contribution statement

Yuan Fu: Conceptualization, Data curation, Investigation, Methodology, Writing – original draft. **Chuanhao Liu:** Formal analysis. **Xiaohui Yan:** Resources, Software. **Guochuan Jiang:** Investigation. **Qiao Dang:** Data curation. **Liyan Wang:** Project administration, Writing – review & editing. **Xuejun Liu:** Funding acquisition.

Declaration of Competing Interest

The authors declare that they have no known competing financial interests or personal relationships that could have appeared to influence the work reported in this paper.

Data availability

The data that has been used is confidential.

Acknowledgments

Appendix A. Supplementary data

Supplementary data to this article can be found online at https://doi.org/10.1016/j.fochx.2022.100484.

References

Ahmad, M., Malik, Singh, C., & Saini. (2018). Heat treatment of sunflower protein isolates near isoelectric point: effect on rheological and structural properties. Food Chemistry. 10.1016/j.foodchem.2018.10.060.

Boer, J. D., Schsler, H., & Aiking, H. (2020). Fish as an alternative protein - a consumer-oriented perspective on its role in a transition towards more healthy and sustainable diets. *Appetite, 152*, Article 104721. https://doi.org/10.1016/j.appet.2020.104721

Brishti, F. H., Yea, C. S., Muhammad, K., Ismail-Fitry, M. R., & Saari, N. (2020). Effects of drying techniques on the physicochemical, functional, thermal, structural and rheological properties of mung bean (*Vigna radiata*) protein isolate powder. *Food Research International, 138*(Pt B), Article 109783. https://doi.org/10.1016/j.foodres.2020.109783

Cho, S. H., Sohn, W. M., Shin, S. S., Song, H. J., & Choi, T. G. (2006). Infection status of pond smelts, *Hypomesus olidus*, and other freshwater fishes with trematode metacercariae in 6 large lakes. *Korean Journal of Parasitology, 44*(3), 243.

Ceng, J., & Liu, X. J. (2014). Study on processing technology of grilled *Hypomesus olidus* pallas. *Meat Industry, 02*, 13–16. https://doi.org/10.3969/j.issn.1008-5467.2014.02.004

Chen, X., Li, P. J., Nishiumi, T., Takumi, H., Suzuki, A., & Chen, C. G. (2014). Effects of high-pressure processing on the cooking loss and gel strength of chicken breast actomyosin containing sodium alginate. *Food and Bioprocess Technology, 7*(12), 3608–3617. https://doi.org/10.1007/s11947-014-1368-9

Chen, Y. J., Ma, M. H., & Fu, X. (2019). Changes in physicochemical properties of protein in vinegar-egg emulsion processing. Modern Food Science and Technology, 35(3), 80-86,206. 10.13982/j.mfst.1673-9078.2019.3.013.

Cc, A., Cs, A., Hl, B., & Rs, A. (2020). Jackfruit (*Artocarpus heterophyllus lam*) leaf as a new source to obtain protein hydrolysates: Physicochemical characterization, techno-functional properties and antioxidant capacity - sciencedirect. *Food Hydrocolloids, 112*. https://doi.org/10.1016/j.foodhyd.2020.106319

Du, H., Zhang, J., Wang, S., Manyande, A., & Wang, J. (2022). Effect of high-intensity ultrasonic treatment on the physicochemical, structural, rheological, behavioral, and foaming properties of pumpkin (*Cucurbita moschata duch.*)-seed protein isolates. *LWT, 155*, Article 112952. https://doi.org/10.1016/j.lwt.2021.112952

FAO/WHO (2007). Protein and amino acid requirements in human nutrition. Report of a Joint WHO/FAO/UNU Expert Consultation, WHO technical report series no.935. Geneva, Switzerland: World Health Organization. i9241209356.

Foh, M., Wenshui, X., Amadou, I., & Jiang, Q. (2012). Influence of pH shift on functional properties of protein isolated of tilapia (*Oreochromis niloticus*) muscles and of soy protein isolate. *Food & Bioprocess Technology, 5*(6), 2192–2200. https://doi.org/10.1007/s11947-010-0496-0

Gong, K. J., Shi, A. M., Liu, H. Z., Liu, L., Hu, H., Adhikari, B., et al. (2016). Emulsifying properties and structure changes of spray and freeze-dried peanut protein isolate. *Journal of Food Engineering, 170*(3), 3–40. https://doi.org/10.1016/j.jfoodeng.2015.09.011

Gou, M. X., Wang, L. Y., & Liu, X. J. (2017). Anticoagulant activity of a natural protein purified from *Hypomesus olidus*. *Natural Product Research, 31*(10). https://doi.org/10.1080/14786419.2016.1222382

Hu, X. Z., Cheng, Y. Q., Fan, J. F., Lu, Z. H., Yamaki, K., & Li, L. T. (2010). Effects of drying method on physicochemical and functional properties of soy protein isolates. *Journal of Food Processing and Preservation, 34*, 520–540. https://doi.org/10.1111/j.1745-4549.2008.00357.x

Heffernan, S., Giblin, L., & O'Brien, N. (2021). Assessment of the biological activity of fish muscle protein hydrolysates using in vitro model systems. *Food Chemistry, 359*, Article 129852. https://doi.org/10.1016/j.foodchem.2021.129852

Kumarakuru, K., Reddy, C. K., & Haripriya, S. (2018). Physicochemical, morphological and functional properties of protein isolates obtained from four fish species. *Journal of Food Science and Technology, 55*. https://doi.org/10.1007/s13197-018-3427-0

Liu, J., Tian, T. T., Tong, J. M., & Zhang, J. (2016). Effect of protein oxidation on physicochemical properties of proteins in *Esox Lucius. The Food Industry, 235*(4), 46–50. CNKI:SUN:SPGY.0.2016-04-013.

Li, Z. Y., Wang, J. Y., Zheng, B. D., & Guo, Z. B. (2020). Impact of combined ultrasound-microwave treatment on structural and functional properties of golden threadfin bream (*Nemipterus virgatus*) myofibrillar proteins and hydrolysates - sciencedirect. *Ultrasonics Sonochemistry, 65*. https://doi.org/10.1016/j.ultsonch.2020.105063

Liu, X. Y., Wang, M. Z., Xue, F., & Benu, A. (2022). Application of ultrasound treatment to improve the technofunctional properties of hemp protein isolate. *Future Foods, 6*, Article 100176. https://doi.org/10.1016/j.fufo.2022.100176

Li, J. P., Fu, J. F., Ma, Y., He, Y. T., Fu, R. X., Abdul, Q., et al. (2022). Low temperature extrusion promotes transglutaminase cross-linking of whey protein isolate and enhances its emulsifying properties and water holding capacity. *Food Hydrocolloids, 125*, Article 107410. https://doi.org/10.1016/j.foodhyd.2021.107410

Martens, H., Stabursvik, E., & Martens, M. (1982). Texture and colour changes in meat during cooking related to thermal denaturation of muscle proteins. *Journal of Texture Studies*. https://doi.org/10.1111/j.1745-4603.1982.tb00885.x

Mune, M. A. M., & Sogi, D. S. (2016). Emulsifying and foaming properties of protein concentrates prepared from cowpea and Bambara bean using different drying methods. *International Journal of Food Properties, 19*(2), 371–384. https://doi.org/10.1080/10942912.2015.1023399

Mehdi, A., & Ingrid, U. (2018). Structural, functional, and sensorial properties of protein isolate produced from salmon, cod, and herring by-products. *Food & Bioprocess Technology, 11*(9), 1733–1749. https://doi.org/10.1007/s11947-018-2138-x

Mignino, L. A., & Paredi, M. E. (2006). Physico-chemical and functional properties of myofibrillar proteins from different species of molluscs. *LWT-Food Science and Technology, 39*(1), 35–42. https://doi.org/10.1016/j.lwt.2004.12.004

Mu, T., Cheng, J. J., Wang, H., Xie, Q. G., Wei, Q. S., & Guo, M. R. (2022). Effects of polymerized goat milk whey protein on physicochemical properties and microstructure of recombined goat milk yogurt. *Journal of Dairy Science, 105*, 4903–4914. https://doi.org/10.3168/jds.2021-21581

Navarro-Lisboa, R., Herrera, C., Zúñiga, R. N., Enrione, J., Guzmán, F., Matiacevich, S., et al. (2017). Quinoa proteins (*Chenopodium quinoa Willd.*) fractionated by ultrafiltration using ceramic membranes: The role of pH on physicochemical and conformational properties. *Food and Bioproducts Processing, 102*, 20–30. https://doi.org/10.1016/j.fbp.2016.11.005

Nieves, H., María, R. R., María, C. V., & Ramon, C. (2022). Influence of high-pressure processing and varying concentrations of curing salts on the color, heme pigments and oxidation of lipids and proteins of Iberian dry-cured loins during refrigerated

storage. *LWT - Food Science and Technology, 160*, Article 113251. https://doi.org/10.1016/j.lwt.2022.113251

Pires, C., Costa, S., Batista, A. P., Nunes, M. C., Raymundo, A., & Batista, I. (2012). Properties of protein powder prepared from Cape hake by-products. *Journal of Food Engineering, 108*(2), 268–275. https://doi.org/10.1016/j.jfoodeng.2011.08.020

Saito, T. (1983). Effect of thermal treatment on extraction of proteins from meats. *Bulletin of the Japanese Society for the Science of Fish, 49*(10), 1569–1597. https://doi.org/10.2331/suisan.49.1569

Shaviklo, G. R., Thorkelsson, G., & Arason, S. (2010). The influence of additives and frozen storage on functional properties and flow behaviour of fish protein isolated from haddock (*Melanogrammus aeglefinus*). *Turkish Journal of Fisheries and Aquatic Sciences, 10*, 333–334.

Shevkani, K., Singh, N., Rana, J. C., & Kaur, A. (2014). Relationship between physicochemical and functional properties of amaranth (*Amaranthus hypochondriacus*) protein isolates. *International Journal of Food Science and Technology, 49*, 541–550. https://doi.org/10.1111/ijfs.12335

Shilpashree, B., Arora, S., Chawla, P., & Tomar, S. (2015). Effect of succinylation on physicochemical and functional properties of milk protein concentrate. *Food Research International, 72*, 223–230. https://doi.org/10.1016/j.foodres.2015.04.008

Shevkani, K., Singh, N., Kaur, A., & Rana, J. C. (2015). Structural and functional characterization of kidney bean and field pea protein isolates: a comparative study. *Food Hydrocolloids, 43*, 679–689. https://doi.org/10.1016/j.foodhyd.2014.07.024

Shen, P., Gao, Z., Xu, M., Ohm, J. B., & Chen, B. (2020). The impact of hempseed dehulling on chemical composition, structure properties and aromatic profile of hemp protein isolate. *Food Hydrocolloids*, 105889. https://doi.org/10.1016/j.foodhyd.2020.105889

Shen, X. L., Li, T., Li, X. H., Wang, F. X., Liu, Y. L., & Wu, J. H. (2022). Dual cryoprotective and antioxidant effects of silver carp (*Hypophthalmichthys molitrix*) protein hydrolysates on unwashed surimi stored at conventional and ultra-low

frozen temperatures. *LWT, 153*, Article 112563. https://doi.org/10.1016/j.lwt.2021.112563

Sahar, S. Y., Marta, S. S., May-Helen, H., Thea, M., Sofie, R., Pedro, A., et al. (2022). Impact of dietary zinc and seawater transfer on zinc status, availability, endogenous loss and osmoregulatory responses in Atlantic salmon smolt fed low fish meal feeds. *Aquaculture, 549*, Article 737804. https://doi.org/10.1016/j.aquaculture.2021.737804

Thorarinsdottir, K. A., Arason, S., Geirsdottir, M., Bogason, S. G., & Kristbergsson, K. (2002). Changes in myofibrillar proteins during processing of salted cod (*Gadus morhua*) as determined by electrophoresis and differential scanning calorimetry. *Food Chemistry, 77*(3), 377–385. https://doi.org/10.1016/S0308-8146(01)00349-1

Tang, X. D., Zhou, C. X., Hong, P. X., & Liu, S. C. (2011). Isolation and characterizing of *Tilapia* proteins. *Food Science and Technology, 6*, 156–159. https://doi:10.13684/j.cnki.spkj.2011.06.050.

Tang, X. D., (2011). Solation and characterizing of Tilapia proteins. (Doctoral dissertation, Guangdong Ocean University). https://kns.cnki.net/KCMS/detail/detail.aspx?dbname=CMFD2012&filename=1012273722.nh.

Yang, H., Chen, D. J., Chen, H. T., & Dong, M. R. (2020). Characteristics of proteins isolated from Giant Salamander muscle. *Meat Research, 34*(7), 28–32. https://doi.org/10.7506/rlyj1001-8123-20200515-121

Yang, J., Huang, F. H., Huang, Q. D., Ma, D., Chen, Y. S., Peng, D. F., et al. (2022). Physical and emulsifying properties of pea protein: Influence of combined physical modification by flaxseed gum and ultrasonic treatment. *Food Science and Human Wellness, 12*, 431–441. https://doi.org/10.1016/j.fshw.2022.07.045

Zhu, G. B., Li, Y. Q., Xie, L., Sun, H. Z., Zheng, Z., & Liu, F. R. (2022). Effects of enzymatic cross-linking combined with ultrasound on the oil adsorption capacity of chickpea protein. *Food Chemistry, 383*, Article 132641. https://doi.org/10.1016/j.foodchem.2022.132641